

X-ray diffraction measurements of the c-axis Debye-Waller factors of $\text{YBa}_2\text{Cu}_3\text{O}_7$ and $\text{HgBa}_2\text{CaCu}_2\text{O}_6$

C. Kim^{1,2}, A. Mehta¹, D.L. Feng^{3,4}, K.M. Shen³, N.P. Armitage³, K. Char⁵, S.H. Moon⁶, Y.Y. Xie⁷, and J. Wu⁷

¹*Stanford Synchrotron Radiation Laboratory, Stanford, California 94309*

²*Institute of Physics and Applied Physics, Yonsei University, Seoul, Korea*

³*Department of Physics and Applied Physics, Stanford University, California 94305*

⁴*Department of Physics, Fudan University, Shanghai 200433, People's Republic of China*

⁵*School of Physics and Center for Strongly Correlated Materials Research, Seoul National University, Seoul 151-742, Korea*

⁶*LG Electronics Institute of Technology, Seoul 137-724, Korea and*

⁷*Department of Physics and Astronomy, University of Kansas, Lawrence, Kansas 66045*

(Dated: November 11, 2018)

We report the first application of x-rays to the measurement of the temperature dependent Bragg peak intensities to obtain Debye-Waller factors on high-temperature superconductors. Intensities of $(0, 0, l)$ peaks of $\text{YBa}_2\text{Cu}_3\text{O}_7$ and $\text{HgBa}_2\text{CaCu}_2\text{O}_6$ thin films are measured to obtain the c-axis Debye-Waller factors. While lattice constant and some Debye-Waller factor measurements on high T_c superconductors show anomalies at the transition temperature, our measurements by x-ray diffraction show a smooth transition of the c-axis Debye-Waller factors through T_c . This suggests that the dynamic displacements of the heavy elements along the c-axis direction in these compounds do not have anomalies at T_c . This method in combination with measurements by other techniques will give more details concerning dynamics of the lattice.

PACS numbers: PACS numbers: 74.25.-q, 61.10.Eq, 74.25.Kc

The majority of efforts to understand the mechanism of the high T_c superconductivity (HTSC) have been in terms of pure electronic effects, primarily because of the conjecture that electron-phonon coupling alone cannot give such a high T_c . However, there have been persistent efforts to study the role of the lattice in HTSC^{1,2,3,4,5,6,7}. In addition to the fact that the structural information provides important information about the materials, the lattice can still play an important role as it affects both the hopping (t) and magnetic exchange (J) energies of these materials, the two most important parameters in the physics of these correlated systems. Indeed, there have been theoretical efforts to study the role of lattice vibration in the cuprates^{1,2}. Therefore, experimental investigation of the temperature dependent lattice vibration in these materials, especially the critical behavior around T_c , is essential and can provide vital information concerning the low energy degrees of freedom.

Experimental evidence that shows clear correlation between the critical behaviors in the electronic and crystal structures are anomalies in lattice constants at T_c . These have been observed in various HTSC materials by x-ray^{3,4} and more accurately by capacitance dilatometry methods^{5,6,7}. They have shown that the lattice constant generally decreases at a much faster rate at T_c than at other temperatures as the temperature decreases. Subsequently, the thermal expansion coefficient α shows an anomaly that is of similar shape to the heat capacity anomalies observed at T_c . This enhanced decrease in the lattice constant has been related to the specific heat capacity through the thermodynamic Ehrenfest relations⁷. Yet the microscopic reason behind such a lattice anomaly is not well understood. One natural question is if it is re-

lated to the dynamic properties of phonons. It will therefore be interesting to measure the Debye-Waller factors (DWF) of HTSC materials.

In complex materials, the DWFs are usually measured by extended x-ray absorption fine structure (EXAFS). In the HTSCs there have been efforts to measure the temperature dependent mean-square displacement $\sigma^2(T)$ (which is inversely related to the DWF) by EXAFS^{8,9,10}, with essentially only Hg based samples showing anomalies at T_c ¹⁰. EXAFS measures local coordinates at a certain atom and therefore has an important advantage of being element specific. It, however, measures only relative atomic motions (for example, O relative to Cu or optical phonons in the Cu-O plane) and is insensitive to collective motions of the atoms, for instance, the low frequency acoustic phonons. To see the effect in the phonon population, the necessary condition is to have ample phonons in the first place. This may be difficult for optical phonons as their energy scale is usually very high compared to the experimental temperature scales (which are set by T_c). This may be related to the fact that EXAFS results largely show no anomalies. In contrast, even though they have their own disadvantages which will be discussed later, diffraction techniques in principle measure the integrated phonon effects¹¹. Here we report novel application of x-ray diffraction that can in principle measure DWFs. This is to our knowledge the first application of this method by x-rays to complex materials like HTSCs. We have measured the temperature dependence of the Bragg peak intensities, a quantity that can be related to the dynamic lattice motion. The results are discussed along with various aspects of x-ray diffraction and possible future experiments.

The experiments were performed at beamline 2-1 of the Stanford Synchrotron Radiation Laboratory (SSRL) which is equipped with a 2-axis Huber diffractometer. The diffractometer has an open cycle He cryostat. $h\nu = 8.8$ keV x-rays, just below the Cu K edge, were used to reduce the background from the fluorescent light. For the reasons explained below, intensities of the $(0, 0, l)$ peaks of $\text{YBa}_2\text{Cu}_3\text{O}_7$ (YBCO) and $\text{HgBa}_2\text{CaCu}_2\text{O}_6$ (Hg1212) thin film samples grown on SrTiO_3 substrates were taken. These materials were grown according to the procedures described elsewhere^{12,13}. The YBCO film has T_c of 90.5K with the ΔT_c less than 1K. The Hg1212 sample has the ΔT_c less than 1K locally but shows distribution of T_c 's from 123K at the center to 118K at the edge.

In order to obtain highly reliable intensities, it is essential to reduce the errors from the beam and sample instabilities and detector non-uniformity. The beam drifts were monitored in the I_0 section and corrected for before each measurement. The biggest effect came from the motion of the cryo-head during the temperature cycle. To reduce such effects, a special manipulator has been designed as shown in Figure 1. The sample holder is in weak thermal contact with the cryo-head and has its own temperature sensor and heater. The thermal contact is weak enough so that the temperature of the sample holder can be varied between 10 K and 200 K with the temperature of the cryo-head maintained at 10 K. This removed most of the sample motion and greatly improved the reproducibility of the data.

The special manipulator did not completely remove the sample motion with respect to the beam during temperature cycling. If the sample was completely homogeneous then the relative motion of the sample will have no effect on the measurement. In our experience, the only high T_c samples which are homogeneous to a highly collimated and monochromatic synchrotron beam are fine grain powders. However, in a powder sample the high index peaks, the peaks more sensitive to the DWF (as $\text{DWF} \sim l^2$), were too weak to measure with sufficient statistical accuracy in a reasonable amount of time. Even though the intensities of the high index Bragg peaks were acceptable in a single crystal we discovered, after looking at high T_c single crystals from several different sources, that these samples were really a bundle of several low angle grain boundary crystallites. Even a small motion of such a sample with respect to the incident beam changed the fraction of the diffracting domain in the beam, which resulted in a significant change in the diffracted beam intensity. Thin films of sufficiently high quality and lateral homogeneity for synchrotron measurements were available but they were all $(0, 0, l)$ orientation¹⁴. Hence, as a compromise between high intensity and sufficiently homogeneous samples, we performed our measurements on the $(0, 0, l)$ peaks of thin film samples.

In addition to the motion of the cryostat upon the temperature change, other factors such as detector non-uniformity contributed to the irreproducibility of the data. Since the effect we were looking for was very small,

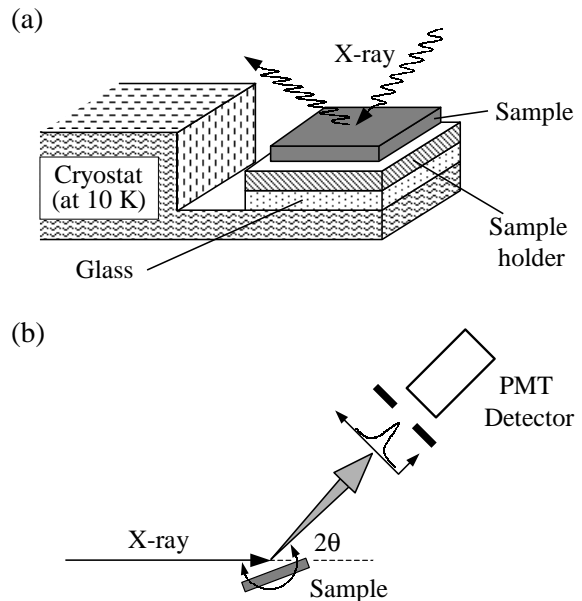


FIG. 1: (a) The schematic of the cryostat designed for the experiments. The sample holder is in weak thermal contact with the cryo-head with its own temperature sensor and heater. Due to the weak thermal contact, the temperature of the sample holder can be varied between 10 K and 200 K while the temperature of the cryo-head fixed at 10 K. (b) Illustration of the experimental configuration. The detector is fixed at the 2θ position while θ is scanned. The detector slit is wide enough to accept the whole Bragg peak as illustrated unlike the conventional setup. The 2θ position is adjusted at each temperature so that the same part of the detector is used.

the accuracy/reproducibility of the measurements had to be better than 0.5%. Therefore, care had to be taken to remove any factor that affects the data quality. The following somewhat unconventional procedure was performed to obtain reliable data. First, the detector slit was set wide enough ($\Delta 2\theta \sim 4$ degrees) to accept all the diffracted x-ray within a certain Bragg peak (Fig. 1). This is to minimize the detector non-uniformity effect as use of angle limiting devices such as Soller slits resulted in very unreliable data. However, some degree of non-uniformity still existed and it was necessary to make it sure that the same part of the detector is used for each scan. To ensure this, we scanned 2θ at each temperature to locate the detector so that the centroid of the diffraction peak is at the center of the detector. In this way, the detector is essentially tracking the temperature dependent motion (in 2θ) of the diffraction peak. As the last step, the θ scans (rocking curves) were taken to measure the diffraction peak intensity. The above procedure produced the most reliable data.

Fig. 2 shows θ scans as well as temperature dependent intensity plots measured as described above. Panel (a) shows normalized θ scans of the $(0,0,13)$ peak from YBCO. The peak position in θ decreases as temperature increases, implying the increase of the c-axis lattice con-

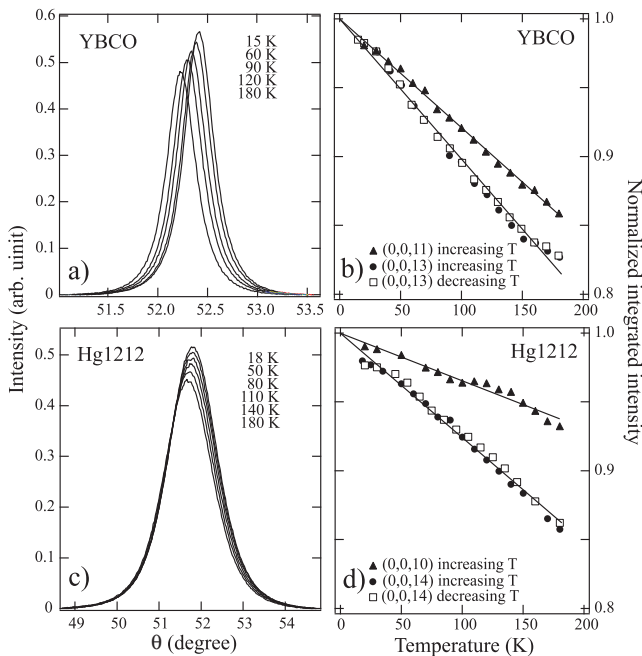


FIG. 2: (a) Series of θ scans of (0,0,13) peak from YBCO at different temperatures. The changes in total intensity as well as the peak position are seen. (b) Temperature vs. integrated intensity plot of the data. The data were taken with the temperature cycled and normalized at $T=0$. Also shown is the data for (0,0,11) peak. (c) Scans of (0,0,14) from Hg1212 samples. (d) Temperature vs. intensity plot for (0,0,14) and (0,0,10) peaks.

stant as expected. In addition to the decrease in the θ position, we note that the Bragg peak intensity decreases as the temperature increases (increased constant background due to incoherent scattering was also observed but subtracted in the plot and analysis). No appreciable change in the diffraction line shape, that is, no q dependence is observed and thus the role of thermal diffuse scattering is not considered in the following discussions. Since the detector slit was wide open (in 2θ) to accept all the x-rays of the peak, each point on the θ scan represents Bragg peak intensity i.e., integration of a 2θ scan at the given θ value. Therefore, the integration of the area represents the sum of the intensities from all the grains of the sample. It is apparent from the figures that the peak intensity decreases as the temperature increases.

To quantify the temperature dependent peak intensities, the peaks shown in Fig. 2a are integrated over the whole angular range. The results are normalized to a common linear extrapolated $T=0$ value and plotted against the temperature in panel (b). For monatomic systems, the intensity of a (0,0, l) Bragg peak is expressed as $I = I_0 \exp(-\frac{1}{2}\langle z^2 \rangle l^2)$ where the exponent is the DWF and $\langle z^2 \rangle$ is the thermally averaged mean square motion of the atoms in z direction¹⁵. For a classical Harmonic oscillator, $\langle z^2 \rangle \propto T$ and the intensity thus becomes $I = I_0 \exp(-\lambda l^2 T) \propto I_0(1 - \lambda l^2 T)$ where λ is a

constant. Therefore, one would expect linear temperature dependence of the DWFs for $T \ll 1/\lambda l^2$. The intensities in the figure show linear temperature dependence and no anomaly is found within the experimental error¹⁶. Also shown in the panel is the temperature dependent intensity of the (0,0,11) peak from YBCO. The ratio of the DWFs of the (0,0,13) and (0,0,11) peaks is 1.28 ± 0.05 which is somewhat close to the expected value of $13^2/11^2 = 1.4$ for monatomic systems with pure thermal phonon effects. The measured temperature dependent intensities suggest normal behavior of the c -axis DWF without any anomaly. Panels (c) and (d) show data from Hg1212 samples. Other than the larger rocking width, the behavior is more or less the same with YBCO case, showing no sign of anomaly at T_c within the experimental error. The deviation of (0,0,10) data from the linear behavior is related to the fact that, unlike other peaks, it was measured along with substrate peaks hence producing larger experimental errors, and is assumed to be extrinsic effect.

Interpretation of the above results, however, is not as easy as the case for monatomic systems such as Si. The expression of a Bragg peak intensity contains in general exponential functions of the displacement parameters of the atoms in the unit cell. For a monatomic case, it could be reduced to a single exponential function of the displacement parameter (assuming the displacement parameters for the atoms in the unit cell are the same) and the DWF can be interpreted with a relative ease. The form factors for polyatomic compounds however are different and the Bragg peak intensity is expressed by a combination of exponential functions. It is therefore very hard to extract the information on the dynamic displacements from DWFs. The other aspect is that the observed temperature dependence does not solely come from the dynamic displacements. Not only the phonons but also the changes in the static atomic positions within the unit cell affect the intensities.

In spite of the difficulties, we can still extract useful information from the results. Even though the Bragg peak intensity expression contains multiple exponential terms, it shows linear temperature dependence if the displacements are purely due to thermal vibrations. Therefore, the fact that experimental data show linear temperature dependence strongly suggests that the major contributor to the DWF is the dynamic displacements as there is no intrinsic reason for such temperature dependence from the static displacements. Indeed, detailed neutron diffraction experiments on YBCO show that the mean square displacements are mostly dynamic¹⁹. We also note that heavy elements contribute more to the diffraction intensities in our x-ray measurements due to their greater high Z sensitivity. To see the different contributions, we list in Table 1 calculated fractions of the planar oxygen and Cu-O planar contributions to the total diffraction peak intensities of YBCO and Hg1212 using the published structural information^{17,18}. Note that the fractions do not add up to make the total due to the in-

Sample	F_c^2 (total)	F_c^2 (Cu-O plane)	F_c^2 (planar O)
YBCO	50.0	2.58	1.00
Hg1212	1386	1.90	1.00

TABLE I: Calculated F_c^2 's for YBCO (0,0,13) and Hg1212 (0,0,14) normalized to plane O values. Cu-O plane and planar oxygen contributions have been calculated with the occupancies of the other atoms set to zero.

terference but roughly show the insignificant Cu-O plane contribution to the total intensity. It is thus conceivable that the phonon anomalies in the Cu-O plane measured by EXAFS¹⁰ may be buried under the contributions from the heavy elements. Based on these, it is reasonable to conclude that at least the heavy elements do not show anomaly at T_c in their c-axis dynamic properties.

On the more fundamental side, the anomalies in the c-axis lattice constants are generally relatively small compared to those along a- or b-axes^{4,6,7}. Therefore, it is possible that the c-axis phonon population anomaly may well be very small and undetectable. Looking at a- and b-axis Debye-Waller factors is therefore essential. This may explain the absence of the anomaly in the Hg1212 data while measurement by EXAFS on powder samples of similar compound $\text{HgBa}_2\text{CuO}_4$ shows anomaly in the mean square displacements¹⁰. Use of Rietveld refinement with powder diffraction at a brighter x-ray source could give an answer to this. Better yet, considering all the factors discussed above, similar experiments by neutron diffraction may resolve most of the problems; the typical grain sizes of HTSC crystals and sample motion upon temper-

ature change are insignificant compared to the neutron beamsizes. This will allow us to investigate a- and b-axis DWFs by a diffraction technique. In addition, its sensitivity to low Z atoms will allow more accurate estimation of the oxygen contribution to the DWFs. There indeed is a strong indication that temperature dependent (1,2,12) neutron Bragg peak intensities of YBCO crystals have anomalies at the T_c ¹⁹.

In conclusion, temperature dependent c-axis DWFs of YBCO and Hg1212 thin films are obtained by measuring the temperature dependent (0, 0, l) x-ray Bragg peak intensities. The measured DWFs show linear temperature dependence within the experimental errors, showing no anomalous effects near T_c . Considering the fact that the x-ray diffraction intensity is much more sensitive to the heavy elements, the results suggest that there is no anomalous lattice dynamics of heavy elements along the c-axis. Further studies of a- and b-axis temperature dependent DWFs by neutron diffraction in combination with temperature dependent structural studies by EXAFS may shed more light on the temperature dependent lattice dynamics, i.e., role of the phonons in HTSCs.

We would like to thank F. Bridges and J. Arthur for helpful discussions, and H. Shin for statistical analysis. SSRL is operated by the DOE office of Basic Energy Research, Division of Chemical Sciences. The office's division of Material Science provided support for this research. This work is supported (in part) by the Korean Science and Engineering Foundation (KOSEF) through Center for Strongly Correlated Materials Research (CSCMR) at Seoul National University.

¹ A. Nazarenko, and E. Dagotto, Phys. Rev. B **53**, 2987 (1996).
² T. Sakai, D. Poilblanc, and D. J. Scalapino, Phys. Rev. B **55**, 8445 (1997).
³ H. You, U. Welp, and Y. Fang, Phys. Rev. B **43**, 3660 (1991).
⁴ T. Asahi, H. Suzuki, M. Nakamura, H. Takano, and J. Kobayashi, Phys. Rev. B **55** 9125 (1997).
⁵ K. Kadowaki, F. E. Kayzel, and J. J. Franse, Physica C **153-155**, 1028 (1988).
⁶ M. Braden, O. Hoffels, W. Schnelle, B. Büchner, G. Heger, B. Hennion, I. Tanaka, and H. Kojima, Phys. Rev. B **47**, 12288 (1993).
⁷ V. Pasler, P. Schweiss, C. Meingast, B. Obst, H. Wühl, A. I. Rykov, and S. Tajima, Phys. Rev. Lett. **81**, 1094 (1998).
⁸ C. Y. Yang, S. M. Heald, J. M. Tranquada, A. R. Moodenbaugh, and Y. Xu, Phys. Rev. B, **38**, 6568 (1988).
⁹ C. H. Booth, F. Bridges, J. B. Boyce, T. Claeson, B. M. Lairson, R. Liang, and D. A. Bonn, Phys. Rev. B **54**, 9542 (1996).
¹⁰ A. Lanzara, N.L. Saini, A. Bianconi, F. Duc, and P. Bordet, Phys. Rev. B, **59**, 3851 (1999).
¹¹ C. Kittel, *Introduction to Solid State Physics*, John Wiley & Sons, Inc., New York, 1986.

¹² B. F. Cole, G.-C. Liang, N. Newman, K. Char, G. Zaharchuk, and J. S. Martens, Appl. Phys. Lett. **61** 1727 (1992).
¹³ J. Z. Wu, S.L. Yan, and Y.Y. Xie, Appl. Phys. Lett. **74** 1469 (1999).
¹⁴ a- or b-axis YBCO thin films do exist. However, these films are grown on LaSrGaO_4 substrates which have a cubic structure. The result is that the substrate peaks, which are much stronger, overlap with the peaks from the film, making those film sample useless for our experiments.
¹⁵ This formula holds true only for monatomic systems. For polyatomic compounds, it is more complicated. See the discussion that follows later in the text.
¹⁶ The fluctuations in Fig 2b and 2d are not from the statistical shot noise in the counts but are mostly due to the extrinsic effects such as the thermal motion of the sample as discussed in the text. The size of the error bar based on our experience is 0.5% or less. All of the root mean square errors of the data are less than 0.5%.
¹⁷ J. D. Jorgensen, B. W. Veal, A. P. Paulikas, L. J. Nowicki, G. W. Crabtree, H. Claus, and W. K. Kwok, Phys. Rev. B, **41**, 1863 (1990).
¹⁸ For Hg1212, published atomic positions of $\text{TlBa}_2\text{CaCu}_2\text{O}_7$ which is isostructural with Hg1212 were used. For

TlBa₂CaCu₂O₇ structure, see B. Morosin, D. S. Ginley, P. F. Hlava, M. J. Carr, R. J. Baughman, J. E. Schirber, E. L. Venturini, and J. F. Kwak, *Physica C* **152**, 413 (1998).

¹⁹ P. Schweiss, W. Reichardt, M. Braden, G. Collin, G. Heger, H. Claus, and A. Erb, *Phys. Rev. B*, **49**, 1387 (1994).